Anodic bonding using a hybrid electrode with a two-step bonding process*

Luo Wei(罗巍), Xie Jing(解婧), Zhang Yang(张阳),
Li Chaobo(李超波)†, and Xia Yang(夏洋)

Key Laboratory of Microelectronics Devices & Integrated Technology, Institute of Microelectronics, Chinese Academy of Sciences, Beijing 100029, China

Abstract: A two-step bonding process using a novel hybrid electrode is presented. The effects of different electrodes on bonding time, bond strength and the bonded interface are analyzed. The anodic bonding is studied using a domestic bonding system, which carries out a detailed analysis of the integrity of the bonded interface and the bond strength measurement. With the aid of the hybrid electrode, a bubble-free anodic bonding process could be accomplished within 15–20 min, with a shear strength in excess of 10 MPa. These results show that the proposed method has a high degree of application value, including in most wafer-level MEMS packaging.

Key words: wafer bonding; anodic bonding; electrode configuration; bubble-free
DOI: 10.1088/1674-4926/33/6/066001 **EEACC:** 2575

1. Introduction

Wafer bonding is a common process used in micro-electromechanical systems (MEMS), microelectronics and optoelectronics[1−3]. In the past few decades, various bonding techniques have already been developed, such as silicon-to-silicon fusion bonding, silicon-to-glass anodic bonding, and intermediate layer bonding. The anodic bonding of glass and silicon is an important step for the fabrication and packaging of MEMS devices. It is a kind of direct bonding technology, with a good hermetic seal, high bond strength and low residue stress. Anodic bonding is suitable for the packaging of micro devices which demand isolation from their operating environments[4], or to meet the *in-situ* physical observation needs of biological samples.

The major challenges of large area silicon-to-glass anodic bonding using existing bonding techniques are the removal of bubbles (unbonded areas), the high bonding strength of the interface and high efficiency. Therefore, different complex types of electrodes, such as line cathodes and multiple-point cathodes, have been reported in recent years[5−7, 10]. It is well known that if a single-point cathode is used to bond a large area wafer, it may take a long time to finish wafer level bonding, but trapped bubbles across the wafer are minimized. If a large planar cathode electrode is chosen to contact a glass wafer as large as the whole glass area, the bonding time may be reduced. However, it would be easier for gas bubbles to become trapped in the bonded interface[8−10].

To take advantage of the planar electrode and point electrode, based on our bonding equipment, this paper proposes to combine the two simplest cathodes to constitute a hybrid electrode to reduce the bonding time and form a bubble-free interface. The two-step anodic bonding process is discussed, and the bond strength and interface integrity of using different types of electrode are determined.

2. Experiment

Anodic bonding has been accomplished using a domestic wafer level bonding system as shown schematically in Fig. 1. The bonding setup accommodates up to 100 mm size wafers. It comprises a DC power supply, electrodes, temperature controlled workstations, a pressure vessel, a servo system and a vacuum chamber. A highly flexible point-shaped electrode supplies a contact force and a DC voltage on the wafers at the first step. Then the planar anodic bonding was performed with the help of a servo motor system, which precisely controls the position of the bottom bond head.

The silicon wafers used in anodic bonding were 4 inch, boron doped (100) standard bare wafers with a resistivity of

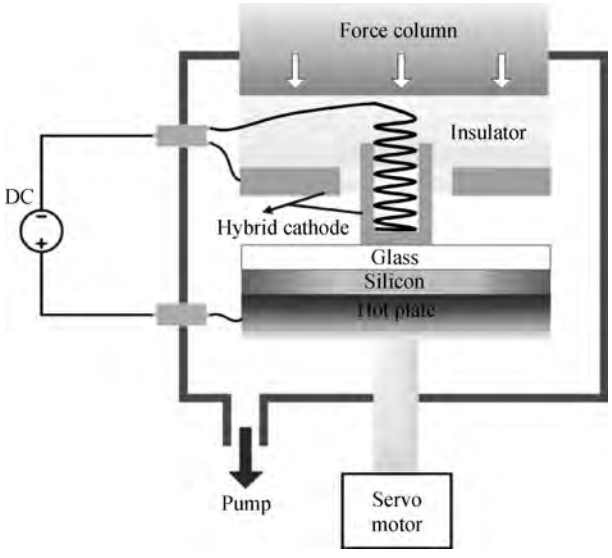

Fig. 1. Schematic diagram of the wafer level bonding setup.

* Project supported by the Development Project of the Scientific Equipment of the Chinese Academy of Sciences (No. YZ200940).
† Corresponding author. Email: lichaobo@ime.ac.cn
Received 12 December 2011

Table 1. List of anodic bonding experiments and their processing conditions.

Electrode type	Voltage (V)	Temp. (℃)	Spring force/External pressure (0.1 MPa)	Vacuum (MPa)	Time (min)	Efficiency	Quality
Point	800	300	SF	5	30	Low	Bubble-free
Planar	800	300	EP	5	30	High	Several bubbles
Hybrid	800	300	SF followed by EP	5	30	High	Bubble-free

8–12 Ω·cm. The glass wafers used were 4 inch Pyrex 7740 borosilicate glass wafers. The thickness of both the silicon and glass wafers was of the order of 500 μm, and they were cleaned in an ultrasonic bath by acetone and deionized water prior to bonding.

Typically, the bonding process is performed by heating a glass and silicon sandwich to a typical temperature of 300–500 ℃ across which a DC voltage of 400–1200 V is applied[11, 12]. Since the main purpose of this paper is to investigate the effects of the type of electrodes on anodic bonding, the bonding temperature, voltage, bonding time and vacuum level were set identically to ensure accurate comparisons.

The integrity of the bonded interface was characterized by scanning electron microscopy (SEM) and energy dispersive X-ray analysis (EDAX). The bond strength measurement was performed using a Dage 4000 bond tester, and the crack section of the bonded sample was studied under OLYMPUS@ MX61 microscopy.

3. Results and discussion

To achieve a bubble-free interface of the Si/glass, different types of electrodes were systematically investigated. Table 1 shows a list of the experiments performed in this study. With respect to the hybrid electrode configuration, the bonding process includes two processes, where primarily the wafers move up to contact intimately with the central pin. There is an air cushion between the contact clearances of the pairs. Obviously, the upper wafer appears to become gently warped under the stress of the deformed highly flexible point-shaped electrode. Once the voltage and temperature reach, the single-point electrode bonding process starts, and a gray region appears below the point electrode.

With the help of high vacuum conditions and expanded bonding front, the air gap and the trapped bubbles between the wafers are squeezed out, as shown in Fig. 2(a). Then, after 10 min, the servo motor moves up until the planar electrode meets the surface of the wafers. Figure 2(b) clearly shows the following step when an external pressure of 0.1 MPa is applied to the samples, and the DC power supply switch is connected from the point cathode to the planar cathode. The bonding process is accomplished within 20 min.

Figure 3 shows optical and SEM images of the Si/glass specimens anodically bonded using the single-point cathode, the planar cathode, and the hybrid cathode under the conditions listed in Table 1. The upper plate is the Pyrex 7740 and the lower one is silicon. In the case of single-point cathode anodic bonding in Fig. 3(a), after bonding for 30 min, part of the area is still unbonded. It is also observed that the bonded area radically diffuses from the site of the cathode to the edge of the wafers, and there are no bubbles in the silicon/glass bonded area. The dashed line (1) again shows that the glass and silicon

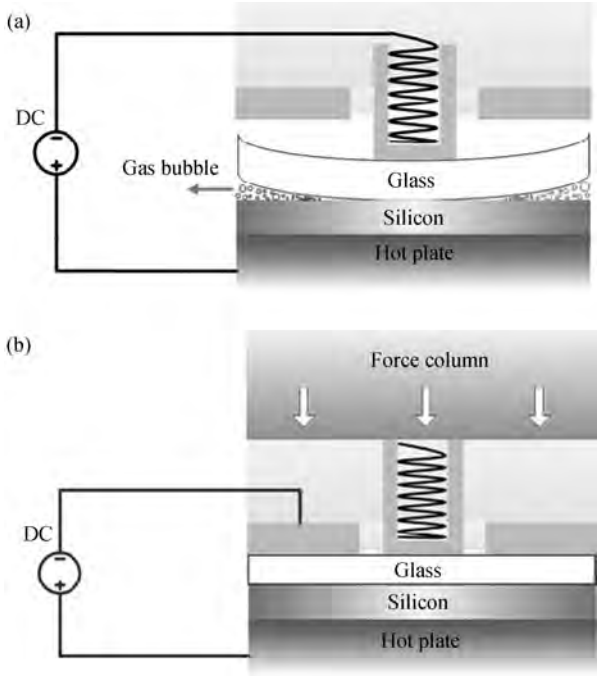

Fig. 2. The hybrid cathode anodic bonding process. (a) For the single-point cathode, gas bubbles are expelled out substrate contact interface under vacuum conditions and through spreading of the bonding front. (b) A large area and rapid bonding process is achieved after the use of the force column and the planar cathode.

are densely bonded together. Figure 3(b) and dashed line (2) show that although the almost full area is successfully bonded, it can be seen that some gas bubbles are trapped at the bonded interface caused by the simultaneous bonding processes occurring at each zone of the interface, and that the gas within the interface has no way to get out. A bubble-free interface is achieved at the hybrid electrode configuration as shown in Fig. 3(c) and dashed line (3). So this type of electrode can improve the interface integrity.

The thin layers of silicon oxide are formed at the bonded interfaces by anodic bonding, as shown in dashed line (1) in Fig. 3(a) and dashed line (3) in Fig. 3(b). EDAX results are shown in Fig. 4. And in the results, oxygen, sodium, aluminum and silicon are found. Comparing the two results, it can be concluded that the sodium content is found to be sharply reduced at the bonded interfaces, and the depletion layers are formed at the side of the bulk glass due to the migration of sodium under applied DC voltage and high temperature[13].

Silicon to glass bonding takes place immediately when the external voltage is applied. Figure 5 shows the current–time relationship under the hybrid electrode configuration. At the beginning of the bonding process, the single-point electrode is at work. The initial peak current comes up to 1.7 mA, and

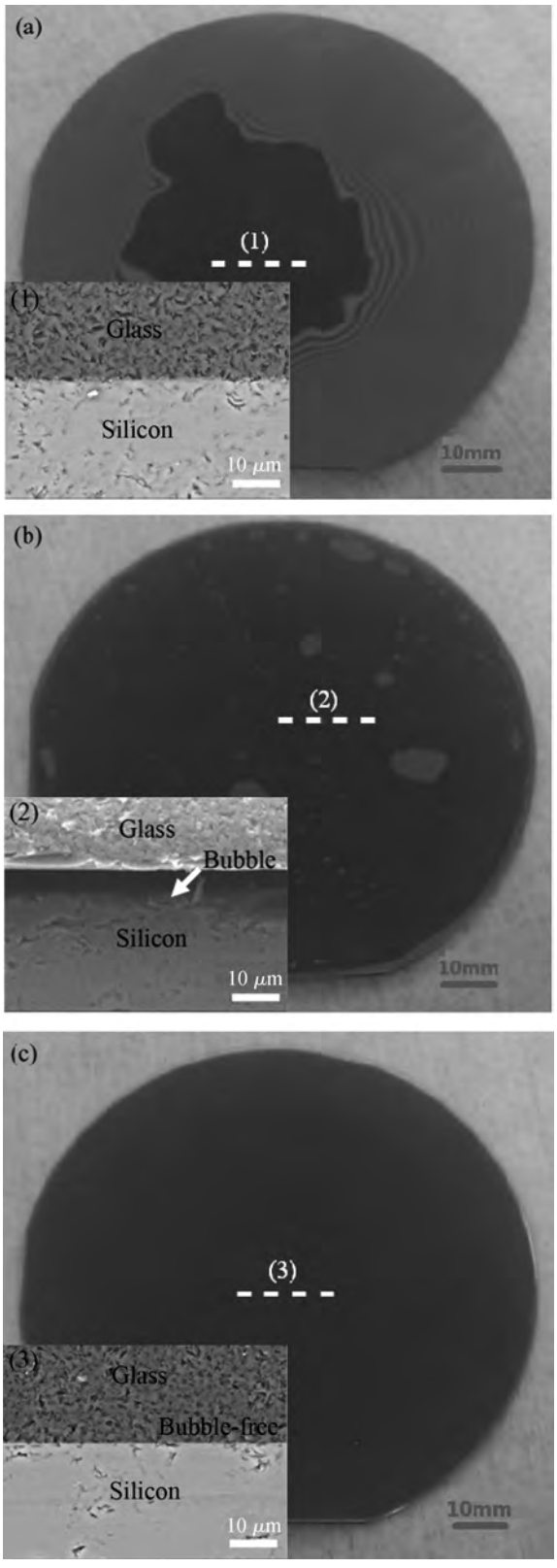

Fig. 3. Optical images of the silicon to glass wafers anodically bonded under (a) the single-point cathode, (b) the planar cathode, and (c) the hybrid cathode. The SEM pictures of the cross-sections of the bonded pairs (1)–(3) correspond to dashed lines (1)–(3), respectively in (a), (b) and (c).

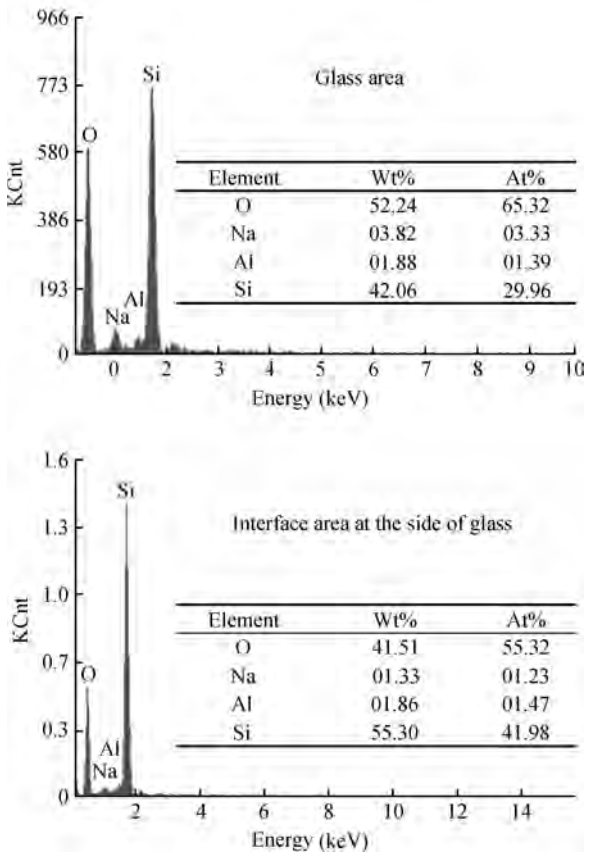

Fig. 4. EDAX measurement results.

then drops slowly until the equilibrium state is established. According to the distributed parameters model of point cathode, the electrostatic pressure between bonding wafers varies with bonding front and time. The farther from the point cathode, the larger the electrostatic is. But as time goes on, the peak electrostatic force will diffuse from the central pin to the surrounding area[14, 15]. Consequently, under this process, the bonded region spreads radically outwards from a spot beneath the point cathode, and the trapped gas bubbles are squeezed out by the propagation of the bonding front, which could result in a bubble-free bonded interface. However, the single-point case takes too long. The propagation velocity $\mathrm{d}R_\mathrm{F}/\mathrm{d}t$ of the anodic bonding front can be expressed as[16]

$$\frac{\mathrm{d}R_\mathrm{F}}{\mathrm{d}t} = \left[\rho C \frac{\sqrt{(R_\mathrm{F}-a)^2+h^2}}{R_\mathrm{F}-a}\left(1+\ln\frac{R_\mathrm{F}}{a}\right) - \rho C \frac{h^2/(R_\mathrm{F}-a)^2}{\sqrt{(R_\mathrm{F}-a)^2+h^2}} R_\mathrm{F} \ln\frac{R_\mathrm{F}}{a}\right]^{-1}, \quad (1)$$

where ρ is the resistivity of the glass, C is the capacitance per unit area of the glass–silicon interface, R_F is the radius of the bonding front, h is the thickness of glass, and a is the radius of the point electrode. Typically, it would take 1.5 h to finish wafer bonding with a size of four inches in diameter[10].

In the second period, instead of keeping the point electrode in use, the planar electrode is used to accelerate the bonding process. The peak current is much higher than that in the case of the point cathode and decays more quickly. The current

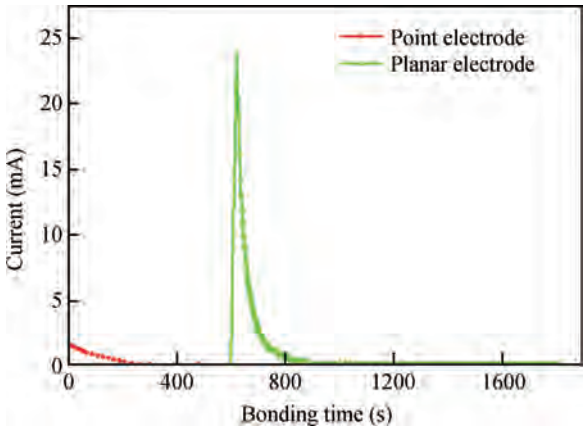

Fig. 5. Current curve of the hybrid cathode anodic bonding process.

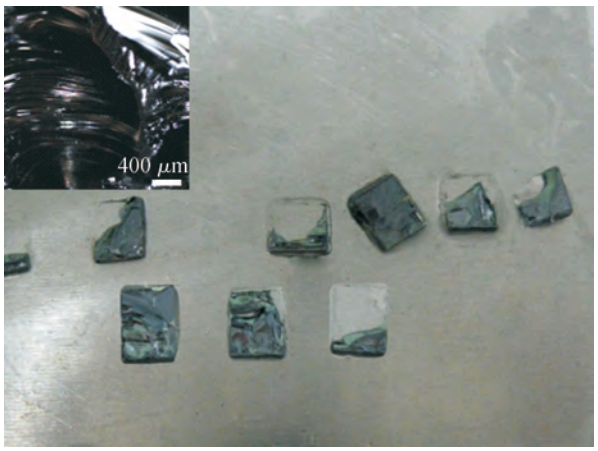

Fig. 6. Cracked samples after the shear test.

maximum is limited to 30 mA to protect the electronic device of the bonding system. The current continues decreasing until the gray color spreads all over the left unbounded region. The whole wafer bonding was done at 800 V for 15–20 min using the hybrid cathode. The results prove that the proposed hybrid cathode can effectively shorten anodic bonding time and improve bonding quality.

To evaluate the hybrid cathode anodic bonding strength, the bonded substrates are cut into several specimens of 4 × 4 mm^2 for shear strength testing. The shear strength of the adhesive we used here is above 10 MPa. Figure 6 shows some typical cracked surfaces by anodic bonding after the shear test. It is obvious that the upper glass fractured instead of the bonding surface dislocation for the majority of the samples. The average measured bonding strength of the specimens left on holders is over 11 MPa.

An optical micrograph of one cracked sample is also shown in Fig. 6. The dark areas in Fig. 6 are where the Si is pulled off from the surface of the Si substrate, showing that fracture occurs within the silicon wafer and that a strong bond which has comparable or higher fracture strength than the bulk silicon has been achieved. This result shows that the bond strength is large enough for most wafer-level MEMS packaging.

4. Conclusion

From experimental analysis, anodic bonding using a hybrid electrode with a two-step bonding process is reported. The design of the hybrid electrode, equipped on the domestic wafer level bonding system, avoids the use of non-standard and complicated electrodes and only combines conventional electrodes. In hybrid cathode anodic bonding, as a first step, trapped gas bubbles are pushed out of the interfaces by using the point cathode under vacuum conditions. The second step is to speed up the bonding process with the help of the planar cathode. The proposed bonding method can therefore achieve high bonding quality compared to using the point cathode alone, but as quickly as the planar cathode anodic bonding process. When bubble-free large area anodic bonding, such as wafer-level packaging, is required, the method presented in this article could provide a good bonding result.

References

[1] Lee B, Seok S, Chun K. A study on wafer level vacuum packaging for MEMS devices. J Micromechan Microeng, 2003, 13(5): 663

[2] Zhu Shiyang, Li Aizhen, Huang Yiping. Transfer of thin epitaxial silicon films by wafer bonding and splitting of double layered porous silicon for SOI fabrication. Chinese Journal of Semiconductors, 2001, 22(12): 1501

[3] Kopp C, Augendre E, Orobtchouk R, et al. Enhanced fiber grating coupler integrated by wafer-to-wafer bonding. J Lightwave Technol, 2011, 29(12): 1847

[4] Tong Q Y, Gösele U. Semiconductor wafer bonding: science and technology. New York: John Wiley & Sons, 1999

[5] Huang J T, Yang H A. Improvement of bonding time and quality of anodic bonding using the spiral arrangement of multiple point electrodes. Sensor and Actuator A, 2002, 102(1): 1

[6] Ito N, Yamada K, Okada H, et al. A rapid and selective anodic bonding method. The 8th International Conference on Solid-State Sensors and Actuators, and Eurosensors IX, Stockholm, Sweden, 1995

[7] Wu Dengfeng, Wu Yuting, Chu Jia, et al. Rapid anodic bonding method with line cathode. Journal of Transducer Technology, 2003, 22(5): 17

[8] Michael H. Electrode for anodic glass bounding on silicon in semiconductor mfr. Patent No. DE 4426288, 1996

[9] Katsumi T, Tomoaki G, Koji M. Anodic bonding methods. Patent No. JP2000-121468A, 2000

[10] Teich M, Marek P, Schmidt A. Substrate anodic bonding electrode arrangement. Patent No. DE 4423164 A1, 1996

[11] Knowles K M, van Helvoort A T J. Anodic bonding. International Materials Reviews, 2006, 51(5): 273

[12] Albaugh K B, Cade P E. Mechanisms of anodic bonding of silicon to pyrex glass. Technical Digest, IEEE Solid-State Sensor and Actuator Workshop, Hilton Head Island, SC, USA, 1988

[13] Lee D J, Ju B K, Jang J, et al. Effects of a hydrophilic surface in anodic bonding. J Micromechan Microeng, 1999, 9(4): 313

[14] Anthony T R. Anodic bonding of imperfect surfaces. J Appl Phys, 1983, 54(5): 2419

[15] Tang Jialu, Liu Xiaowei, Zhang Haifeng, et al. Investigation of electrostatic bonding time model with point cathode. Proceedings of the 4th IEEE International Conference on Nano/Micro Engineered and Molecular Systems, Shenzhen, China, 2009

[16] Zhou Qingchun, Chen Zheng, Dong Shirun. Method of equivalent electrical circuit for point cathode electric field assisted anodic bonding. Transactions of the China Welding Institution, 2002, 23(1): 37